

PAPER • OPEN ACCESS

A battery-to-electrolyzer pathway for energy management in a hybrid battery/hydrogen microgrid

To cite this article: Athar Ahmad *et al* 2023 *J. Phys.: Conf. Ser.* **2648** 012094

View the [article online](#) for updates and enhancements.

You may also like

- [Mass Transfer in Parallel Plate Electrolyzers with TwoPhase LiquidLiquid Flow](#)
PoYen Lu and Richard C. Alkire
- [Evaluation of Anode Porous Transport Layer Using Polarization Separation Method on PEM Water Electrolysis](#)
Taiki Ishida, Kensaku Nagasawa, Yosuke Sano et al.
- [The Illustrated Wavelet Transform Handbook: Introductory Theory and Applications in Science, Engineering, Medicine and Finance](#)
J Ng and N G Kingsbury

PRIME
PACIFIC RIM MEETING
ON ELECTROCHEMICAL
AND SOLID STATE SCIENCE

HONOLULU, HI
Oct 6–11, 2024

Abstract submission deadline:
April 12, 2024

Learn more and submit!

Joint Meeting of
The Electrochemical Society
•
The Electrochemical Society of Japan
•
Korea Electrochemical Society

A battery-to-electrolyzer pathway for energy management in a hybrid battery/hydrogen microgrid

Athar Ahmad, Mario Iamarino and Antonio D'Angola

Scuola di Ingegneria, Università degli Studi della Basilicata, Via dell'Ateneo Lucano 10, 85100 Potenza, Italy

E-mail: athar.ahmad@unibas.it, mario.iamarino@unibas.it, antonio.dangola@unibas.it

Abstract. A RES-based microgrid with two simultaneous storage options - battery and hydrogen - is considered. While the battery pack serves as a short-term storage solution, the hydrogen-cycle (consisting of an electrolyzer, a hydrogen pressurized tank and a fuel cell stack) provides for a long-term (seasonal) storage in order to improve the system resilience and to allow off-grid operation for longer time. With respect to the most classical energy management approach, where energy is transferred either from PV to battery (as the priority transfer) or from PV to electrolyzer, the novel strategy adopted in this paper also adds the possibility of a battery-to-electrolyzer energy conversion route. This route is enabled whenever the energy stored in the battery is expected to overcome the estimated short-term energy needs. The novel strategy reveals significant potential to increase the hydrogen production during the summer months, by redirecting to the electrolyzer part of the excess energy that would be otherwise curtailed or transferred to an external grid. Application of the strategy during autumn and winter time reveals on the contrary a clear worsening of the microgrid performance and should be avoided.

1. Introduction

Renewable energy sources (RES) such as solar and wind power have emerged as an effective solution for addressing the challenges of climate change and energy sustainability [1, 2]. This has led to the development of RES-based microgrids which integrate local generation sources, energy storage systems and smart grid technologies to enhance the reliability, efficiency, and sustainability of energy self-consumption in decentralized settings.

Energy storage plays a crucial role in managing the intermittent nature of renewable energy sources and balancing the supply and demand dynamics, as it allows to store excess energy during periods of high generation and release it during periods of high demand. In this respect, battery storage systems have been widely adopted in microgrids due to their high efficiency, rapid response, and mature technology. However, they come with important limitations such as high costs, limited capacity, degradation and energy losses over time, and environmental concerns related to the extraction and disposal of hazardous materials. To overcome some of these limitations, hydrogen-based energy storage systems have emerged as a potential alternative. Hydrogen has unique advantages as the high energy density and the long-term storage capability, and can therefore provide a reliable and sustainable backup power source especially in isolated off-grid areas. However, the adoption of hydrogen storage in microgrids requires additional infrastructure, including hydrogen production, compression, and storage facilities, and implies



much higher energy losses compared to batteries. In order to combine the advantages of batteries and hydrogen, a promising approach is the integration of both options into a single microgrid which utilizes batteries for short-term storage needs due to their higher efficiency and faster response time, while leveraging hydrogen for long-term storage requirements due to its high energy density and ability to store energy over extended periods [3].

The implementation of an efficient Energy Management System (EMS) is essential to accomplish the aforementioned advantages. In fact, the EMS system plays a crucial role in controlling the energy transfer between the energy sources, the available storage options, the applied load, and the main grid when available. A quite basic EMS strategy (here referred to as Battery First, or B1st) prioritizes the battery for energy storage and retrieval. With this strategy, during periods of energy surplus the excess energy is first stored in the battery until this is fully charged, and if there is still surplus energy available, this is transferred to an electrolyzer to produce and store hydrogen. If the hydrogen tank is full, or the available power exceeds the electrolyzer power, any excess energy is sold to the main grid or curtailed. Conversely, during periods of energy deficit, the battery is discharged first to meet the energy demand. If additional energy is required, a fuel cell stack intervenes by utilizing the stored hydrogen to generate the needed power; if the hydrogen tank is empty or the required power exceeds the fuel cell power, further energy needs will be met by transferring energy from the main grid. In conclusion, this approach preferentially relies on the battery for both energy storage and supply by minimizing the use of the less energy-efficient hydrogen loop. Despite its simplicity, the B1st approach has been widely and successfully adopted in many similar setups [4, 5, 6, 7]. Certain variations to the main idea of the B1st strategy have also been proposed. In [8], in order to reduce the battery pack size, the battery charging has lower priority in allocating the excess energy if the available power is comprised between the minimum and the nominal power of the electrolyzer. In [9], the B1st strategy is directly compared with the opposite approach prioritizing hydrogen production and consumption over batteries; results indicate that the hydrogen-first approach guarantees a more reliable microgrid operation with smaller default time but at the cost of higher energy losses.

More sophisticated EMS approaches for hybrid microgrids with battery and hydrogen storage options include advanced control, forecasting models and optimisation algorithms to determine the most suitable storage policies based on factors such as energy demand, renewable energy generation and system cost considerations. For example, an optimization strategy is used in [10] with the aim of using hydrogen storage to cope with load and irradiance volatility while the battery serves for energy arbitrage with the main grid under dynamic energy pricing conditions. The opposite approach is tackled in [11] in a cost optimisation exercise for a grid-connected microgrid which takes into account also degradation costs for hydrogen cycle components and batteries; here hydrogen is produced when energy prices are low and converted back to electricity when prices are high, while the battery is used for intra-day power balancing.

In existing EMS strategies the battery and hydrogen storage systems are typically operated in parallel. This means that surplus energy flows from PV generation to the load either through the battery pathway or the hydrogen pathway, while the impact of enabling a direct energy exchange between the two storage systems remains relatively unexplored. In order to cover this gap, the present paper aims at investigating the benefits and challenges of adding a battery-to-electrolyzer pathway in hybrid RES-based microgrids, with the aim of utilizing the battery as an intermediary storage device for part of the available energy before this is transferred to the electrolyzer. The EMS strategy which includes such pathway will be referred to as Battery-To-Electrolyzer strategy (or B2el) and has already revealed some good potential based on preliminary observations [4].

The behaviour of the B2el strategy will be investigated during a 1-year simulation of a RES-based residential microgrid assumed to be located in Potenza, Italy (reference year for irradiance

data will be 2016). Results will be compared with those obtained with the more classical B1st strategy, highlighting benefits and drawbacks of the novel approach.

2. Microgrid setup

The microgrid considered in this paper is supposed to be located in the town of Potenza, Italy, at 768 m ASL (40.643° lat. and 15.805° long.). The selected location is classified as 'Csb' according to the Köppen-Geiger climate classification and is characterized by a Mediterranean climate with precipitations mostly concentrated in the autumn and winter, while summers tend to be hot and dry.

The microgrid includes a solar PV system, an electrochemical battery storage, an electrolyzer, a fuel cell stack, a compressed hydrogen tank and voltage converters, as shown in Figure 1. The energy transfer takes place along two separate common buses, one interconnecting the DC devices (PV panels, battery, electrolyzer and fuel cell stack) and one connected to the AC load and possibly to the external grid. An AC/DC converter enables power to flow between the two circuits.

A typical daily residential load profile has been considered, characterized by three different consumption peaks (two during the day and one more pronounced during the evening) followed by lower night demand, as shown in Figure 2. The total energy consumption is 137 kWh/day or 50 MWh/y, reflecting the electricity demand of a small community of domestic consumers.

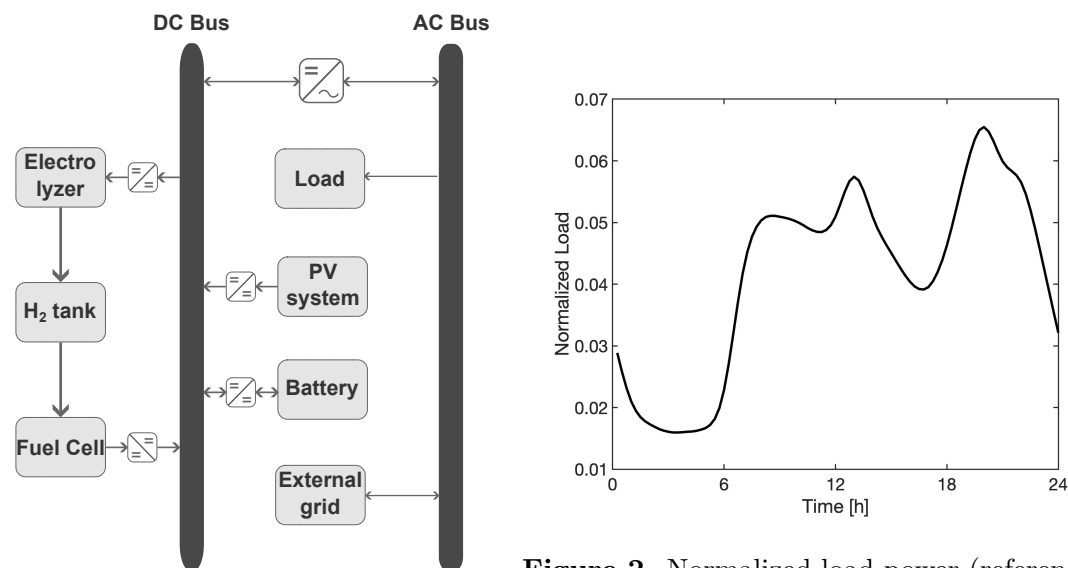


Figure 1. Architecture of the hybrid microgrid.

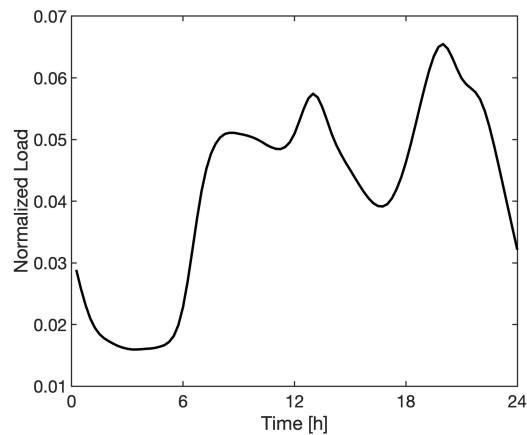


Figure 2. Normalized load power (reference: 1 energy unit consumption per day).

2.1. Photovoltaic system

The individual photovoltaic module has been modelled as an equivalent circuit with a single diode, a series resistance and a shunt resistance [12, 13, 14].

A first order estimation of the minimum PV capacity requirement is carried out assuming that ideally all energy generated by the PV plant in one year (E_{PV}) is directly used to sustain the entire yearly load (E_L). For this, global solar irradiance data for Potenza have been extracted from the PVGIS database for the year 2016, with time resolution of 1 h [15]. The irradiance data refer to a tilt of 33° and an azimuth of -10°, which represent the optimal values for the

given location. The minimum capacity of the PV system is related to the energy produced with the help of the following expression:

$$E_L = E_{PV} = H_g N_{min} S \eta_{STC} PR \quad (1)$$

where H_g is the annual solar irradiation (kWh/m²/year), N_{min} is the minimum number of photovoltaic modules, S is the PV module surface (m²), η_{STC} is the PV system efficiency at Standard Test Conditions which corresponds to an irradiance G_{STC} of 1 kW/m² and cell temperature T_{STC} of 25 °C, and PR is the system performance ratio. With $P_{STC} = G_{STC} S \eta_{STC}$ being the STC nominal power of the module, the minimum number of modules can be calculated starting from eq.(1) as:

$$N_{min} = \frac{E_L G_{STC}}{H_g P_{STC} PR} \quad (2)$$

The system performance ratio PR considers various losses such as temperature losses, module mismatch, aging, light induced degradation and potential induced degradation. This can be evaluated from the following equation:

$$PR = k_T \eta_{PCU} \quad (3)$$

where η_{PCU} is the power conditioning unit losses (assumed here to be 0.86, corresponding to electrical system losses of 14% as recommended by the PVGIS tool), and k_T is the weighted average of the monthly thermal losses $k_{t,i}$,

$$k_T = \sum_{i=1}^{N_m} k_{t,i} \frac{H_{m,i}}{H_g} \quad (4)$$

$$k_{t,i} = (1 + \gamma(T_{c,i} - T_{STC})) \quad (5)$$

in which γ is the power temperature coefficient, $T_{c,i}$ is a conservative estimation of the monthly average cell temperature (see below), and $H_{m,i}$ is the monthly solar irradiation at an inclined plane. The average cell temperature on a monthly basis is estimated as [18]:

$$T_{c,i} = \bar{T}_{max,i} + \frac{T_{NOCT} - 20}{G_{NOCT}} \bar{G}_{max,i} \quad (6)$$

where $\bar{T}_{max,i}$ is the maximum average temperature for the month i , T_{NOCT} is the nominal operating cell temperature, G_{NOCT} is 0.80 kW/m², $\bar{G}_{max,i}$ is the maximum value of the irradiance for the month i assuming a sinusoidal behaviour in which the average monthly irradiance magnitude \bar{G}_i is calculated as

$$\bar{G}_i = \frac{H_{m,i}}{N_{d,i} N_{h,i}} \quad (7)$$

being $\bar{G}_{max,i} = \frac{\pi}{2} \bar{G}_i$, and $N_{d,i}$ and $N_{h,i}$ the number of days and number of daylight hours in the month i .

The photovoltaic module selected for this work has a nominal power of 0.47 kW, a NOCT temperature of 41.5°C and a γ value of -0.29 %/°C. By using these values in eq. 2 one obtains $N_{min} = 77$. The energy losses in the two storage systems and in the energy converters are highly dependant on the particular EMS strategy adopted (which determines the intensity of use of the battery and hydrogen storage) and on the size of the different microgrid components. A reasonable estimation would be 35% of the PV capacity, based on the direct observation of the system behaviour under a variety of relevant conditions. This leads to a final number of PV modules of 104 and to a total nominal installed capacity of 49 kW corresponding to a peak PV generation of approximately 42 kW (after subtracting the mentioned 14% for system losses).

2.2. Storage systems

The Li-ion battery pack has a total capacity of 138 kWh which would be enough to sustain the applied load for one full day in the absence of any other energy source. The power exchanged during charging and discharging is limited by the maximum current of 1 A per cell, introduced in order to preserve battery life; with the particular battery pack configuration adopted, this corresponds to a $P_{B,max}$ of 40 kW, which is however only occasionally reached under the conditions adopted in this study. The Status of Charge (SOC) of the battery is defined as the ratio between the actual energy stored in the battery and the maximum battery storage capacity and ranges from $SOC_{min} = 0.2$ and $SOC_{max} = 1$. The charging process takes place at variable current (capped by the maximum allowable value), which depends on the available PV power at any particular time; once the SOC exceeds the value 0.85, the remaining charge is provided at constant voltage and gradually decreasing current.

Both the electrolyzer and the fuel cell stack are based on Proton Exchange Membrane (PEM) technology, which operates at relatively low temperatures [16]. The fuel cell stack has a maximum power of 9.6 kW, chosen in a way to be always able to sustain the given load (peak load is 9 kW at 8 PM). Therefore, if hydrogen is available, the microgrid never needs to import energy from external grids or to rely on other backup systems.

The electrolyzer has a maximum power of 10 kW, which means it may not always absorb the entire surplus energy available during the day, so that a fraction of this energy often needs to be curtailed or transferred to an external grid. In order to avoid the efficiency drop observed in real systems when the device is fed at a power much lower than its maximum power rating [17], a minimum power has been also applied to the electrolyzer equal to 20% of the maximum. The characteristic voltage-current relationships for the fuel cell stack, the electrolyzer and the battery are those already presented in a previous paper [4].

The SOT (State of Tank) is the indicator used to reflect the relative amount of hydrogen stored at any time in the tank, and its value ranges from $SOT_{min} = 0.05$ to $SOT_{max} = 1$. However, the tank volume has been intentionally oversized compared to the actual capacity requirements in order to avoid that the hydrogen storage capacity becomes a limiting factor for the hydrogen production or consumption. This means that SOT_{max} and SOT_{min} are never reached during the simulations, effectively treating the tank as if it has an infinite volume.

2.3. Energy Management System

The Energy Management System controls the balanced energy transfers between demand, production and storage options. The two EMS strategies adopted in this paper are the classical B1st strategy and the novel B2el strategy.

Operationally, the B1st strategy consists in evaluating, at each time step, the difference P_{diff} between the photovoltaic power P_{PV} and the load P_L . If this is positive, the fuel cell power P_{FC} is set to zero and the surplus energy is used first to recharge the battery at a rate P_B , capped by the maximum battery power $P_{B,max}$. This transfer goes on as long as $SOC < SOC_{max}$. Any additional available energy is transferred to the electrolyzer with rate P_{EL} (limited by the maximum and minimum electrolyzer powers, $P_{EL,min}$ and $P_{EL,max}$), as long as $SOT < SOT_{max}$. If there is residual power exceeding the permissible electrolyzer power range, or in case the hydrogen tank is full, available energy is eventually curtailed or transferred to an external grid (P_G), if present. On the contrary, when P_{diff} is negative, the energy needs are sustained in cascade by discharging the battery at a rate $P_{B,d}$ (capped by $P_{B,max}$) as long as $SOC > SOC_{min}$, and any additional energy need will be sustained by the fuel cell stack at a rate P_{FC} (capped by $P_{FC,max}$). If there is still energy demand above the fuel cell stack maximum power, or if there is no hydrogen in the storage tank, energy needs must be met by importing from an external grid (P_G), if present.

The B2el strategy adds an extra step to the B1st strategy that is exclusively activated during

nighttime. In particular, at each time t between midnight and sunrise time t_s , the EMS evaluates the available energy in the battery as a function of the current SOC and battery capacity C_B :

$$E_{av} = C_B(SOC - SOC_{min}) \quad (8)$$

as well as the energy required to sustain the load during the night and up to one hour after sunrise:

$$E_{need} = \int_t^{t_s+1} P_L dt \quad (9)$$

If $E_{av} > E_{need}$, a surplus of energy is available in the battery and this is transferred from the battery to the electrolyzer at a rate P_{B2el} which is upper-limited by the device with the lower maximum available power (for the battery, available maximum power will be $P_{B,max} - P_L$, while for the electrolyzer it is $P_{EL,max}$). The transfer goes on until one of the conditions $E_{av} > E_{need}$ or $t < t_s$ is no longer met, after which the P_{B2el} power is set to zero and the energy management system reverts to the standard B1st strategy.

The choice to enable the battery-to-electrolyzer energy transfer only at night has two main advantages: on one side, the electrolyzer can focus during the day entirely on converting PV energy without diverting any of its available power to the battery-to-electrolyzer transfer, on the other side it takes advantage of the considerably more stable and easily predictable night load compared to the strong variability of the daytime electricity consumption. Moreover, the energy needs during the night are evaluated until one hour after sunrise to better cope with the uncertainties associated with the early morning hours when the PV generation may not be sufficient to fully cover the morning load. This is particularly important in winter when irradiance is low and sunrise occurs later, i.e. when energy demand is already ramping up due the morning peak in the load profile. It is also important to point out that the different parameters of the B2el strategy (such as the starting time and the duration of the the battery-to-electrolyzer transfer, or the power to be allocated to the transfer, etc.) are not optimized but have been selected based on general considerations, and that the night load is estimated in the ideal case of no uncertainties in the knowledge of the load profile.

3. Results and Discussion

A comparison of the two energy management strategies is presented in this section under three different weather scenarios (referred to as scenario A, B and C) which adequately catch - to the purpose of this analysis - the range of relevant weather conditions that may be encountered throughout the year. The focus is on hydrogen production and the overall performance of the microgrid over two consecutive days for each weather condition and strategy.

The first scenario (A) corresponds to stable weather characterized by clear skies and medium-to-high irradiance, as commonly encountered during summer when such conditions may last for weeks or even months; other seasons may also experience this type of weather but with lower probability and shorter duration. With a proper sizing of the microgrid components, a significant amount of surplus energy $P_{PV} - P_L$ is usually available and sufficient to fully charge the battery (P_B) and produce hydrogen in the electrolyzer (P_{EL}), while any residual energy exceeding the electrolyzer power must be curtailed or transferred to the external grid, if present (P_G). This is the case of Figure 3.[A0] obtained with the B1st strategy: here the battery SOC always experiences values above 0.55 as the battery is only used to sustain the modest load at night and quickly recharges to $SOC = 1$ in the early morning hours, followed by the activation of the electrolyzer up to its maximum power. When applying the B2el strategy (Figure 3.[A1]), an additional energy transfer (P_{B2el}) from the battery to the electrolyzer takes place during the night to convert into hydrogen any unused energy available in the battery; this causes the SOC to approach the minimum (0.2) in a discharging process controlled by the EMS which makes sure

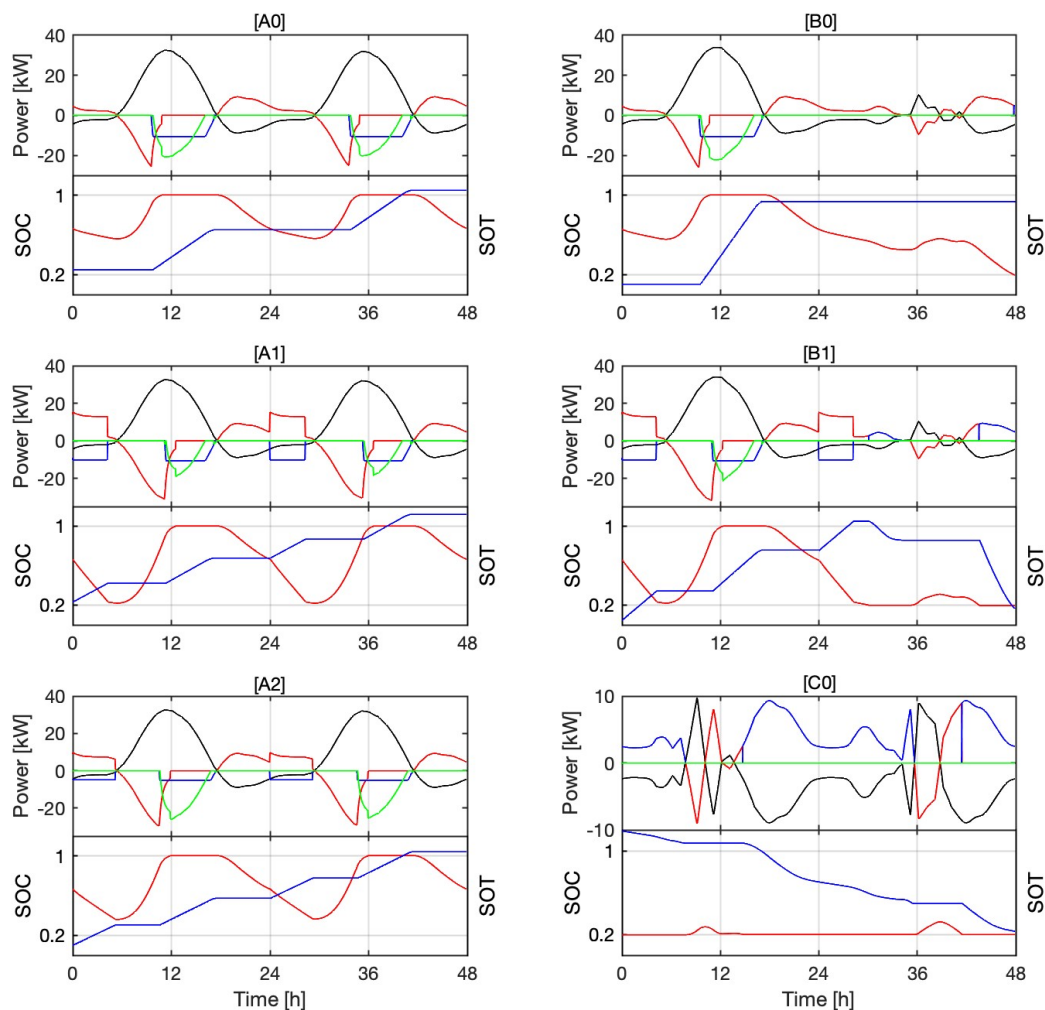


Figure 3. Upper charts: Power exchanged between microgrid components (black line: $P_{PV} - P_L$; red: P_B ; blue: $P_{FC} + P_{EL}$; green: P_G) under different weather scenarios (A: summer months; B: intermediate seasons; C: winter months) and EMS strategies (0: B1st; 1,2: B2el). Lower charts: State of Charge (SOC, red line) and State of the hydrogen Tank (SOT, blue line) for each combination of weather scenario and strategy.

there is always enough energy left in the battery to sustain the load until one hour after sunrise. This additional energy transfer results in a higher total production of hydrogen over the two days (+35%), compared to the B1st strategy, achieved by diverting to the electrolyzer part of the energy that would be otherwise curtailed, which in turn decreases by -38%. Interestingly, this can be achieved without modifying the size of any microgrid component. A possible variation from the [A1] case is when the night battery-to-electrolyzer energy transfer is limited by factors others than the minimum battery SOC (such as the limited electrolyzer or battery maximum power, or the shorter duration of the night in summer which reduces the available hours for the transfer). In this case, the lowest SOC reached by the battery before sunrise may be higher, for example around 0.37 as in the case of Figure 3.[A2] obtained by lowering the electrolyzer power from 10 kW to 5 kW, but still the hydrogen production will benefit - albeit to a lesser extent - from applying the strategy.

For scenario (B), variable atmospheric conditions are considered with a first day characterized by clear sky and full irradiance, followed by a second cloudy day with much lower irradiance values. Such conditions may be encountered at any time of the year, although with higher frequency in autumn and spring. During the first day, both strategies allow the battery to reach the maximum SOC and the electrolyzer to produce a similar amount of hydrogen. The B2el strategy however discharges the battery almost entirely during the following night, so that there is no energy left to sustain the load during the second day which is, as said, characterized by low PV production, hence causing the activation of fuel cell stack with consumption of stored hydrogen (Figure 3.[B1]). On the contrary, since with the B1st strategy the battery is not fully discharged during the night, there is enough stored energy to cope with the energy deficit of the second day (Figure 3.[B0]). Consequently, there is no need (or less need, in other similar cases) for fuel cell energy generation and this makes the B1st approach consume less hydrogen in these two days compared to the B2el. The final hydrogen balance of the B2El strategy over the two days is still positive but with a net production which is 81% lower than the one obtained with the B1st approach, despite the decrease of 34% of the curtailed energy.

The last scenario (C) is represented by two consecutive days both characterized by very low irradiance, as frequent in winter months. Regardless of the energy management strategy applied, the battery is only partially charged during both days, and the majority of the load must be sustained by the fuel cell relying on the consumption of stored hydrogen. There is therefore no residual energy available for operating the electrolyzer either during the day or during the night. This results always in a negative hydrogen balance without notable difference between the two strategies, which are therefore both qualitatively described by the behaviour in Figure 3.[C0].

One of the most significant features of implementing the B2el strategy is the more intensive use of the battery compared to the B1st strategy. This is reflected by the histograms in Figure 4, which illustrate the probability distribution of SOC values for both the B1st and B2el strategies during a summer month (July) and a late-autumn month (November). In July, the SOC values for the B1st strategy remain almost exclusively above 0.5 primarily because the need to resort to the battery is minimal in this time of the year. The B2el strategy, on the contrary, keeps draining energy from the battery at night to produce additional hydrogen, and this results in more widely distributed SOC values within the entire allowable range of 0.2 to 1. Interestingly, while the most frequent SOC value is 1 for both strategies, the B2el lowers the associated probability from 0.33 to 0.24, hence leaving the battery in fully charged conditions for less time and better exploiting the available storage capacity. In November the differences in the shape of the SOC probability distribution function are less pronounced. The most frequent value in both cases is 0.2 (battery at its minimum charge), but the B1st approach experiences such conditions with lower probability (0.20) compared to the B2el (0.26). This confirms the earlier observations regarding the superior performance of the former strategy during transitional seasons.

A more detailed analysis on seasonal behaviour and effectiveness of the two EMS strategies is represented in Figure 5, which reports the difference in the monthly hydrogen balances between the B2el and the B1st strategy for the year 2016. The typical omega-shaped behaviour obtained by this analysis is representative of the scenarios previously discussed. The well developed central maximum proves the advantages of using the B2el strategy during the summer months (which are dominated by scenario (A)), as it enables higher hydrogen production by reducing the amount of energy that would otherwise be curtailed or sold to the grid. Such advantages are achieved without requiring any significant changes or additions to the size or capacity of the microgrid components. The difference becomes negative, i.e. more favourable to the B1st strategy, when considering early spring and autumn months as they experience weather conditions with a prevalence of scenario (B). Here, the B1st approach proves more effective since it can rely on generally higher battery SOC values to sustain the load during frequent periods of low irradiance and reduces therefore the hydrogen consumption in the fuel cell stack. A relative maximum can

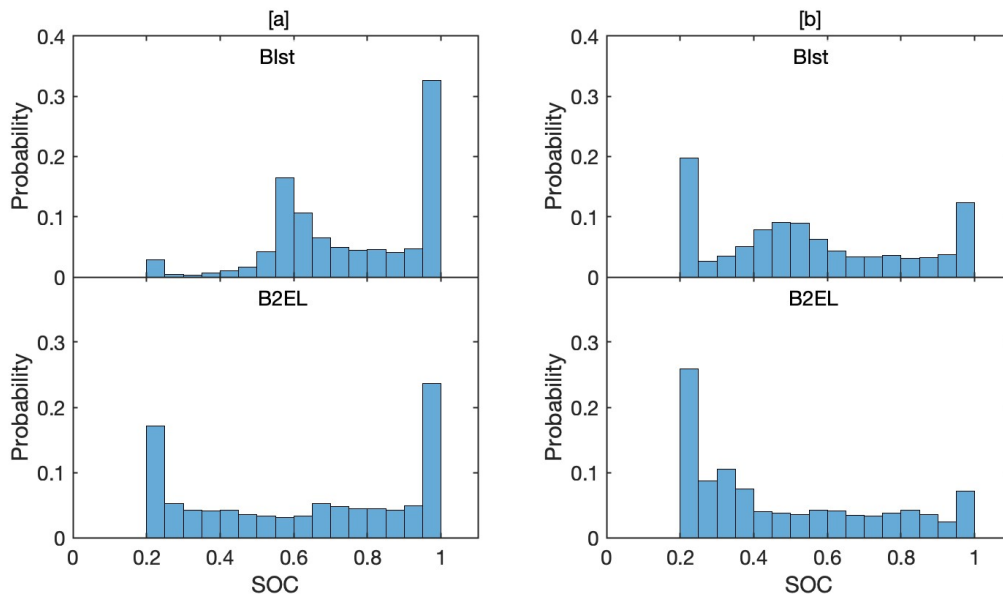


Figure 4. Histograms for the probability distribution of the battery *SOC* in July 2016 [a] and November 2016 [b] for the two strategies.

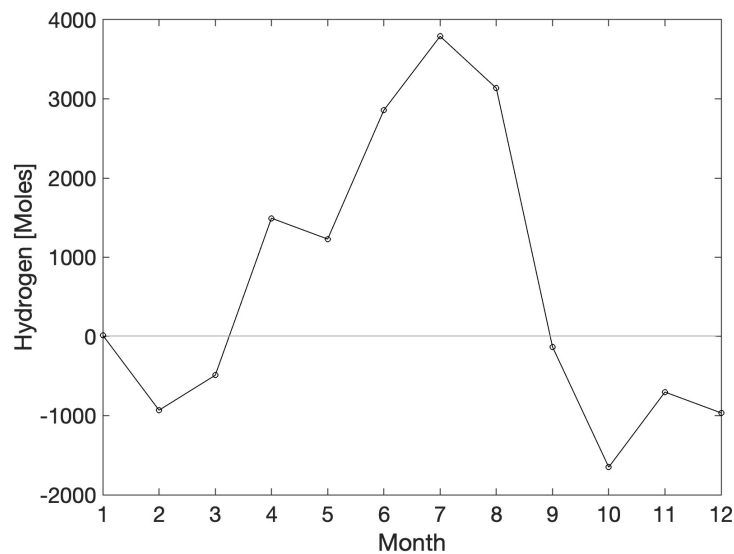


Figure 5. Difference in monthly hydrogen balance between the B2el and the B1st strategy for the year 2016.

be observed in January where the curve touches the zero; this indicates the impact of prolonged low irradiance conditions in winter (scenario C) which tend to be completely insensitive to the particular strategy and therefore nullifying any difference between the two.

The results presented above suggest that a possible combination of the two strategies (i.e., B2el during the late spring and summer months and B1st during the autumn and winter months) could prove as the best solution for maximising the hydrogen production in the microgrid

over the entire year. This in turn opens the way to an improvement of the overall microgrid reliability especially in off-grid scenarios, and of a possible cost cutting concerning the microgrid components. Further investigations are underway to explore such combined approach and to quantify the related advantages.

4. Conclusions

This paper demonstrates the potential advantages of introducing a battery-to-electrolyzer energy exchange route (B2el strategy) to a basic EMS control algorithm with storage options only operated in parallel (B1st strategy). The B2el strategy uses part of the battery capacity as temporary storage during daily PV energy peaks for a certain amount of excess energy which is then transferred to the electrolyzer during the night. This energy transfer takes place under the supervision of an EMS system which, based on a load-forecasting algorithm, ensures that the battery retains sufficient energy to support the load until sunrise. The obtained results show clear and consistent advantages of the B2el strategy over the B1st approach in late spring and summer months, in terms of higher hydrogen production, while the contrary happens in autumn and winter months. Such behaviour has been linked to the predominance of particular weather scenarios in the different months, and the opportunity to switch from one strategy to the other during the year has been recommended.

Acknowledgments

The valuable contribution of Antonello Damato to the conceptualization of the B2el strategy is gratefully acknowledged.

This work was funded by the Next Generation EU - Italian NRRP, Mission 4, Component 2, Investment 1.5, call for the creation and strengthening of 'Innovation Ecosystems', building 'Territorial R&D Leaders' (Directorial Decree n. 2021/3277) - project Tech4You - Technologies for climate change adaptation and quality of life improvement, n. ECS0000009. This work reflects only the authors views and opinions, neither the Ministry for University and Research nor the European Commission can be considered responsible for them.

References

- [1] Greenhouse Gas Emissions from Energy 2023 *IEA* <https://www.iea.org/data-and-statistics/data-product/greenhouse-gas-emissions-from-energy>
- [2] Materi S., D'Angola A., Enescu D., Renna P. 2021 *Production Engineering* **15:5** 667 - 681
- [3] Thakkar N and Paliwal P 2023 *International Journal of Green Energy* **20:4** 445-463
- [4] Damato A, Iamarino M, Ferraro A and D'Angola A 2022 *J. Phys.: Conf. Series* **2385** 012119
- [5] Marocco P, Ferrero D, Gandiglio M, Ortiz M M, Sundseth K, Lanzini A and Santarelli M 2020 *Energy Convers. Manag.* **211** 112768
- [6] Marocco P, Ferrero D, Lanzini A and Santarelli M 2022 *Journal of Energy Storage* **46** 103893
- [7] Castañeda M, Cano A, Jurado F, Sanchez H and Fernandez L M 2013 *International Journal of Hydrogen Energy* **38** 3830-3845
- [8] Serra F, Lucariello M, Petrollese M and Cau G 2020 *Energies* **13** 4149
- [9] Monforti Ferrario A, Vivas F J, Manzano F S, Adujar J M, Bocci E and Martirano L 2020 *Electronics* **9(4)** 698
- [10] Hemmati R, Mehrjerdi H and Bornapour M 2020 *Renewable Energy* **154** 1180-1187
- [11] Fan F, Zhang R, Xu Y and Ren S 2022 *CSEE Journal of Power and Energy Systems* **8** 369-379
- [12] De Soto W, Klein S A and Beckman W A 2006 *Solar Energy* **80(1)** 78-88
- [13] Spertino F., D'Angola A., Enescu D., Di Leo P., Fracastoro G.V., Zaffina R. 2016 *Solar Energy* **133** 119 - 140
- [14] D'Angola A., Zaffina R., Enescu D., Di Leo P., Fracastoro G.V., Spertino F. 2016 *51st International Universities Power Engineering Conference* 1 - 6
- [15] Huld T, Müller R and Gambardella A 20012 *Solar Energy* **86** 1803-1815
- [16] Sharaf O Z and Orhan M F 2014 *Renewable and Sustainable Energy Reviews* **32** 810-53
- [17] Scheepers F, Sthäler M, Sthäler A, Rauls E, Müller M, Carmo M and Lehnert W 2020 *Energies* **13(3)** 612

- [18] ASTM-Standard E1036, Standard test methods for electrical performance of non concentrator terrestrial photovoltaic modules ad arrays using reference cells. The American Society for Testing and Materials, West Conshohocken, PA, USA,